2009

Integrated Capture and Spectroscopic Detection of Viruses

Crystal A. Vargas
University of Arizona, Tucson, Arizona

Allison A. Wilhelm
University of Arizona, Tucson, Arizona

Jeremy Williams
University of Arizona, Tucson, Arizona

Pierre Lucas
University of Arizona, pierre@email.arizona.edu

Kelly A. Reynolds
University of Arizona, Tucson, Arizona, reynolds@email.arizona.edu

See next page for additional authors

Applied and Environmental Microbiology, Oct. 2009, p. 6431–6440 Vol. 75, No. 20
0099-2240/09/$08.00+0 doi:10.1128/AEM.02036-08

Integrated Capture and Spectroscopic Detection of Viruses[▽]

Crystal A. Vargas,[1] Allison A. Wilhelm,[2] Jeremy Williams,[1] Pierre Lucas,[2] Kelly A. Reynolds,[3]* and Mark R. Riley[1]

Agricultural and Biosystems Engineering,[1] Materials Science and Engineering,[2] and Mel and Enid Zuckerman College of Public Health,[3] The University of Arizona, Tucson, Arizona 85724

Received 2 September 2008/Accepted 17 August 2009

The goal of this work is to develop an online monitoring scheme for detection of viruses in flowing drinking water. The approach applies an electrodeposition process that is similar to the use of charged membrane filters previously employed for collection of viruses from aqueous samples. In the present approach, charged materials are driven onto a robust optical sensing element which has high transparency to infrared light. A spectroscopic measurement is performed using the evanescent wave that penetrates no more than 1 μm from the surface of an infrared optical element in an attenuated total reflectance measurement scheme. The infrared measurement provides quantitative information on the amount and identity of material deposited from the water. Initial studies of this sensing scheme used proteins reversibly electrodeposited onto germanium chips. The results of those studies were applied to design a method for collection of viruses onto an attenuated total reflectance crystal. Spectral signatures can be discriminated between three types of protein and two viruses. There is the potential to remove deposited material by reversing the voltage polarity. This work demonstrates a novel and practical scheme for detection of viruses in water systems with potential application to near-continual, automated monitoring of municipal drinking water.

Despite the application of multibarrier, conventional treatment approaches for municipal water, disease outbreaks associated with tap water continue to occur in the United States (37). An etiological agent is not determined in approximately half of all identified drinking water outbreaks; however, the characteristic symptomatology of the causative agent frequently indicates a viral pathogen. The need for rapid and effective methods of virus collection and detection is apparent for the assurance of water security and water quality and certainly also for medical diagnostics.

Commercial systems exist for continual monitoring of municipal drinking water for parameters such as pH, total organic carbon, turbidity, and salt (electrical conductivity). Biological monitoring schemes are available to quantify bacteria, spores, and parasites based on their size or their light scattering or absorbing properties (2, 3, 9). No such approach is available for viruses, which have a smaller size and present a sizeable health concern. Conventional virus detection methods are performed in an off-line manner. These methods have high specificity but are costly, time-consuming, require significant laboratory preparation, and have difficulties adapting to new emerging viruses.

Development of the best available technology for effective monitoring of viral pathogens is critical for evaluating and maintaining potable water sources, treatment reliability, and posttreatment distribution water quality. Current methods of virus detection in environmental samples are compromised by the presence of inhibitory compounds, such as humic and fulvic acids, and detection of nonviable microbes (PCR) or by toxicity and lengthy assay times (conventional cell culture), conditions often leading to false-positive or false-negative results (23). Although the use of an integrated cell culture/PCR method has been shown to overcome major flaws of each individual method (1, 22, 24), this approach is neither automated nor rapid.

Sampling from water systems (source waters and treated water) for detection of viral pathogens is usually performed with either positively charged membranes, which allow fluid to pass through the filter and collect viruses based on charge, or hollow fiber concentrators, which allow fluid to move across the membrane surface rather than being forced through and concentrate viruses by removal of liquid and larger molecules. In neutral solutions and most environmental drinking water sources, viruses are negatively charged. Adsorption to hollow fiber or filter surfaces is largely due to electrostatic and hydrophobic interactions and is controlled by environmental factors, such as pH and electrolytes (16). Once adsorbed to electrocharged filters, viruses are typically eluted via high-pH buffers or bioflocculants, such as beef extract. Collected materials are then analyzed using culture or primer-specific molecular detection methods. We aim to replace one of these fibers within a hollow fiber concentrator with an optically addressable fiber for spectroscopic detection of viruses deposited using electrophoretic collection, similar in process to commercial electronic air filters.

The long-term goal of the present work is to develop an automatable means to detect viruses in aqueous samples using electrodeposition to capture viruses on the surfaces of optical fibers for infrared spectroscopic characterization and identification. Infrared spectroscopy is noninvasive and can provide information in minutes on the composition of a material. The components of a virus (nucleic acids, proteins, phospholipids, and other small molecules) present distinct vibrational fingerprints in the infrared (10–12) which can be used to identify and

* Corresponding author. Mailing address: The University of Arizona, Zuckerman College of Public Health, Environmental Health Sciences, 1295 N. Martin Ave., Tucson, AZ 85724. Phone: (520) 626-8230. Fax: (520) 626-8009. E-mail: reynolds@u.arizona.edu.

▽ Published ahead of print on 21 August 2009.

quantify the type of virus. Other materials present in typical drinking water systems produce minimal signals.

Since infrared light is low energy (compared to UV or visible light), the sample may be repeatedly probed without causing damage, permitting continual measurement over the deposition process (10, 13). The vibrational spectrum collected provides an infrared signature very specific to each chemical or biological species. Spectra are typically collected over the range of 4,000 to 620 cm^{-1} (2.50 to 16.13 μm), which contains the fundamental vibrations and overtones of many biochemicals, including proteins, nucleic acids, phosphates, ammonia, and lipids. For ease of interpretation, the spectral regions are divided into three zones (29). The first, 3,000 to 2,800 cm^{-1}, contains two primary bands at 2,852 cm^{-1} and 2,922 cm^{-1}, which are attributed to CH_2 asymmetric and symmetric vibrations, respectively. CH_2-containing compounds are present predominantly in long-chain hydrocarbons, such as lipids. The two lower-intensity bands at 2,874 cm^{-1} and 2,960 cm^{-1} correspond to the symmetric and asymmetric CH_3 vibrations, respectively, found in lipids and proteins (25). The second (1,700 to 1,400 cm^{-1}) region contains the amide I (1,690 to 1,630 cm^{-1}) and amide II (1,548 cm^{-1}) features typical of proteins. The third spectral region, between 1,100 and 900 cm^{-1}, contains primarily C—O—C and C—O ring vibrations due to carbohydrates and P═O and P—O—P, representative of nucleic acids and phospholipids (18).

The reason for the use of Fourier transform infrared (FTIR) spectroscopy in remote optical sensing is the recent availability of infrared transmitting fibers with low losses and sufficient chemical durability (13, 14). Chalcogenide glasses are one of very few materials that combine large optical windows in the infrared, low optical losses, chemical durability, and the ability to be drawn into fibers (15, 35). These glasses also have semiconducting properties similar to those of silicon and therefore have the appropriate electrical properties for use as an electrode during electrophoretic collection of negatively charged viruses. In the present work, we demonstrate the proof of concept for an electrophoretic optical sensor using a germanium (Ge) attenuated total reflectance (ATR) crystal with transparency from 2 to 13 μm in wavelength that spans the region of interest for identification of viral species. Ge is also a good semiconductor and can therefore act as both an optical element and an electrode. Charge-based collection and deposition of viruses have been demonstrated for a number of applications, including collection of viruses on sand and FeO particles and in column chromatography (19, 21, 31, 33). To our knowledge, this approach has not been previously applied by combining electrodeposition with infrared analysis.

MATERIALS AND METHODS

Proteins and viruses. For development of the method, three commercially available proteins were used in the first stage of experiments. Bovine serum albumin (BSA), casein, and lysozyme were all obtained from Sigma Chemical Co. (St. Louis, MO). The viruses selected for study included the vaccine strain poliovirus type 1 (LSc-2ab) and the bacteriophage MS2, both obtained from Charles Gerba, the University of Arizona. MS2 stocks were purified using centrifugation at 2,800 × *g* for 10 min followed by filtration through a 0.22-μm filter (Millipore, Billerica, MA). Poliovirus was purified via polyethylene glycol precipitation (Sigma Chemical Co., St. Louis, MO) followed by centrifugation at 2,800 × *g* for 15 min. Polyethylene glycol (9%) and sodium chloride (5.8%) were then added, and the solution was stirred overnight at 4°C to precipitate the virus, followed by centrifugation at 10,000 × *g* for 30 min. The virus pellet was resuspended in 0.01 M phosphate-buffered saline (PBS) and extracted using Vertrel XF solvent (DuPont, Wilmington, DE) with continuous shaking for 15 min and centrifugation at 2,500 × *g* for 15 min. Purified viruses were collected from the upper aqueous layer.

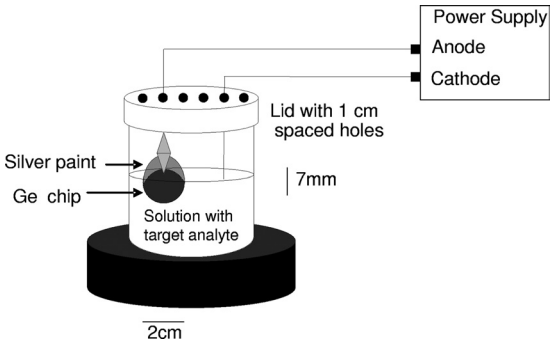

FIG. 1. Electrodeposition setup.

The vaccine strain poliovirus type 1 (LSc-2ab) has been chosen as a model for development of virus concentration, detection, and elution methods. This nonpathogenic enterovirus has been widely utilized as a surrogate for human enteric viruses due to its rapid growth and ease of detection in mammalian cell culture. Decades of research data are published on vaccine strain poliovirus related to surface characteristics, adsorption mechanisms, and other relevant physicochemical properties of the virus (6).

An important component of this detection scheme is premised on the net surface charge carried by the virus. This is gauged by the isolectric point, or pI. Although the data varies with the virus strain and method, poliovirus LSc has a pI of 6.6 and the bacteriophage MS2 has a pI of 3.9. The pIs of the proteins studied are 5.4 for BSA, 4.6 for casein, and 11.0 for lysozyme (5). Compounds have a net positive charge when the pH is below their pI, a neutral charge at the pI, and a negative charge above it. The approach presented here relies upon having net negatively charged viruses, and so the solution pH was maintained around 7.0. Under these conditions, a net negatively charged virus will migrate toward an electrical anode. The pI of lysozyme (pI = 11) is above neutral pH, and thus, the voltage polarity was reversed compared to that used for the other target analytes with a pI below neutral pH. All measurements here were made using tap water with added salts and pH adjustment but with no further purification.

To assess detection limits of the spectroscopic method, FTIR spectra of BSA and poliovirus at various concentrations in Earle's balanced salt solution (minus phosphate) were dried on Ge windows from a 20-μl drop. An FTIR sample holder (constructed of plastic by the Agricultural and Biosystems Engineering machine shop) with a 7-mm-diameter hole was used so that the entire dried material was assessed. A Ge window with a dried 20-μl drop of Earle's balanced salt alone was used as the background. The resulting data were then baseline corrected at 1,800 cm^{-1} and 1,480 cm^{-1}. The amide I (1,656 cm^{-1} [6,039 nm]) and amide II (1,544 cm^{-1} [6,477 nm]) peak heights were also calculated for protein and sugar (1,108 cm^{-1} [5,555 nm]) and acetate (1,018 cm^{-1} [9,823 nm]) for poliovirus (18).

Electrodeposition on Ge chips. In the initial step, proteins and viruses were both tested for electrodeposition using Ge discs obtained from Meller Optics (Providence, RI). A Ge disk was attached to an alligator clip in the electrodeposition setup (Fig. 1), and a 7-mm-long metal wire was used as the cathode. The Ge disk (anode) and the wire (cathode) separation varied from 1 to 5 cm in these experiments. A 50-ml beaker was used to hold the proteins in standard 1× PBS and was placed on a rubber disk. The wire and the Ge disk were connected to a power supply that permitted the voltage to be changed in a controlled manner. Thirty ml of 10 mg/ml of selected protein in PBS was placed in the beaker. The power supply was turned on at the desired voltage and protein deposited. After the power supply was turned off, the Ge disk was removed from the setup and allowed to dry. Upon drying, the deposited material was scanned in the FTIR. Three different spots of the deposited material were scanned for each measurement. In order to estimate the detection limit of these measurements, 20 μl of the protein solutions of decreasing concentrations were also dried on Ge disks. FTIR spectra of the dried solutions were obtained using both a sample holder with a small hole and a sample holder with a large hole. In all scans, a Ge disk was used as the background.

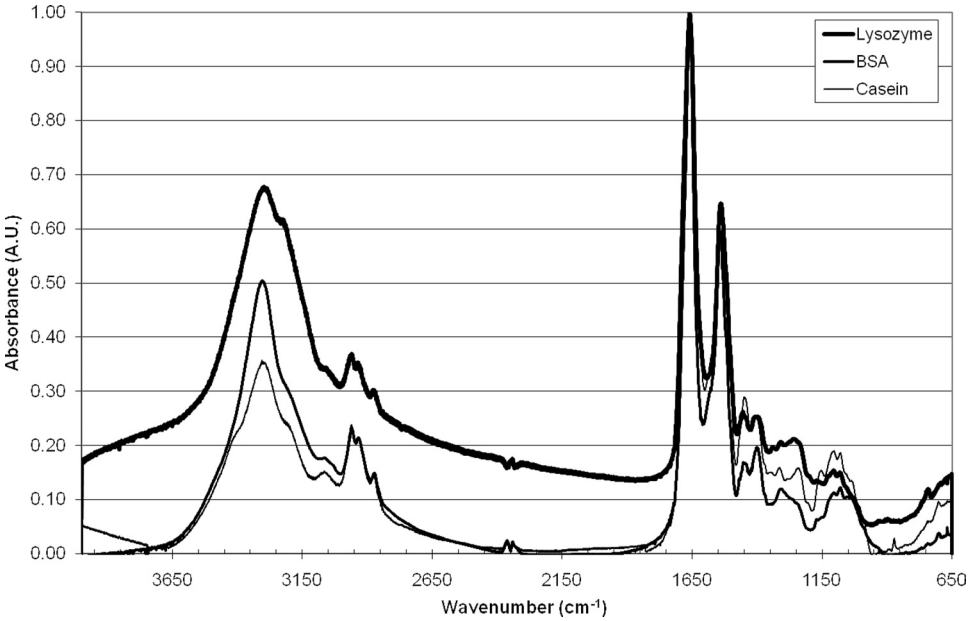

FIG. 2. Spectra of dried powder of the three proteins (BSA, lysozyme, and casein) utilized here.

The Ge disk, with 1/4 of one side painted with silver paint, was used as the anode in this test. The 7-mm-long wire was used as the cathode, and a voltage was applied with a corresponding 1-mA current. The electrodes were kept at a distance of 2 cm. The Ge disks had a resistance of 2.73 kΩ. Temperature was monitored during initial experiments and was found to not increase due to the applied voltage (constant 27.2 ± 0.5°C). Samples were vortexed for 30 s to ensure a well-mixed solution before each electrodeposition. A total of six electrodepositions were performed at 2 cm away at 1 min, 5 min, 10 min, 20 min, and 30 min.

The electrodeposition of the phage MS2 and poliovirus was performed using a Tris buffer (pH 7.23), and a new virus solution was used for each individual electrodeposition onto Ge chips. The Ge disks were dried for 24 h following the electrodeposition at a distance of 2 cm. The initial poliovirus and MS2 seed concentrations were 10^7 PFU/ml for each.

Electrodeposition onto ATR crystal. Electrodeposition was performed with a designed ATR apparatus for use in the FTIR with an applied voltage. A Ge 45-degree trapezoid ATR crystal, purchased from Pike Technologies (Madison, WI), was used both as the wave guide for FTIR/ATR spectroscopy and as an electrode for electrodeposition. Ge was chosen due to its extended transparency window in the infrared and its semiconducting properties. The Ge crystal was placed inside an ATR trough plate fabricated out of nonconductive plastic. A 0.015-in.-thick rectangular polytetrafluoroethylene gasket was placed in between the plastic ATR plate and the Ge ATR crystal to prevent leakage. To improve the electrical contact with the Ge crystal anode, aluminum foil was placed as a cover on the bottom surface of the crystal and held in position by a plastic plate. Approximately 1.8 ml of sample, diluted in tap water, was placed in the trough above the Ge crystal, and on top of this was placed a piece of indium tin oxide (ITO), which served as the cathode. One end of the ITO was covered in silver paint to improve the connection to the power supply. In the most common configuration, the Ge ATR crystal was used as the anode and ITO as the cathode. Applied voltage was typically 1.1 V with a current of approximately 1 mA. ATR spectra were collected at a 2 cm^{-1} resolution using 128 coadded scans. The number of scans was selected as a balance between measurement accuracy and the ability to monitor the deposition over time.

RESULTS

Measurements were performed with solutions of protein or virus pipetted directly onto Ge chips and dried, after which infrared spectra were collected. Figure 2 shows spectra of three proteins; Fig. 3 shows spectra of poliovirus and MS2 bacteriophage. Spectra of lysozyme, BSA, and casein (Fig. 2) had superficial similarities, with strong features at 3,200, 1,650, and 1,550 cm^{-1}. However, upon closer inspection, sizeable differences were apparent, especially within the 1,500 to 1,000 cm^{-1} region, which holds information on sugar content (glycosylation), protein structure (alpha helices versus beta sheets), and phosphorylation.

The two viruses assessed here displayed substantial differences in their spectral fingerprints (Fig. 3). Poliovirus had strong absorbances at 2,886 cm^{-1} (lipids), 1,465 cm^{-1} (lipids), 1,134 cm^{-1} (lipid), 1,108 cm^{-1} (sugars), 962 cm^{-1} (phosphates), and 864 cm^{-1} (ribose). MS2 had strong features at 3,192 cm^{-1} (protein), 1,632 cm^{-1} (protein), 1,296 cm^{-1} (lipids), 1,038 cm^{-1} (sugars), and 665 cm^{-1} (nucleic acids). Note that this classification as "lipids" is based on the standard in spectroscopic analysis but should be more accurately characterized as CH_2 and CH_3 vibrations. These molecules are most commonly found in hydrocarbon chains and categorized broadly as "lipids." We maintain this classification here for consistency and simplicity. This issue is discussed further below. These features are highly distinct but can shift by 1 cm^{-1} based on preparation and spectral collection methods. Spectra of viruses deposited onto Ge chips either by pipetting or by electrodeposition showed no discernible differences (data not shown). Figure 3 indicates that not only are these features distinct for discriminating viruses but they suggest that enough information is present to discriminate between sampled poliovirus or MS2 through use of computation-based analysis tools (7, 26, 30, 32).

Spectral signals for various concentrations of BSA solutions dried on Ge chips showed a linear measurement range between 0.01 and 1 mg/ml and saturation above 2 mg/ml (Fig. 4). Reliable measurements can be made with differences of 0.01 absorbance units, which correspond to 0.1 mg/ml of protein. Correlation coefficients within this range were 0.996 for the amide I feature and 0.996 for the amide II feature, indicating no substantial difference in the quality of measurement when

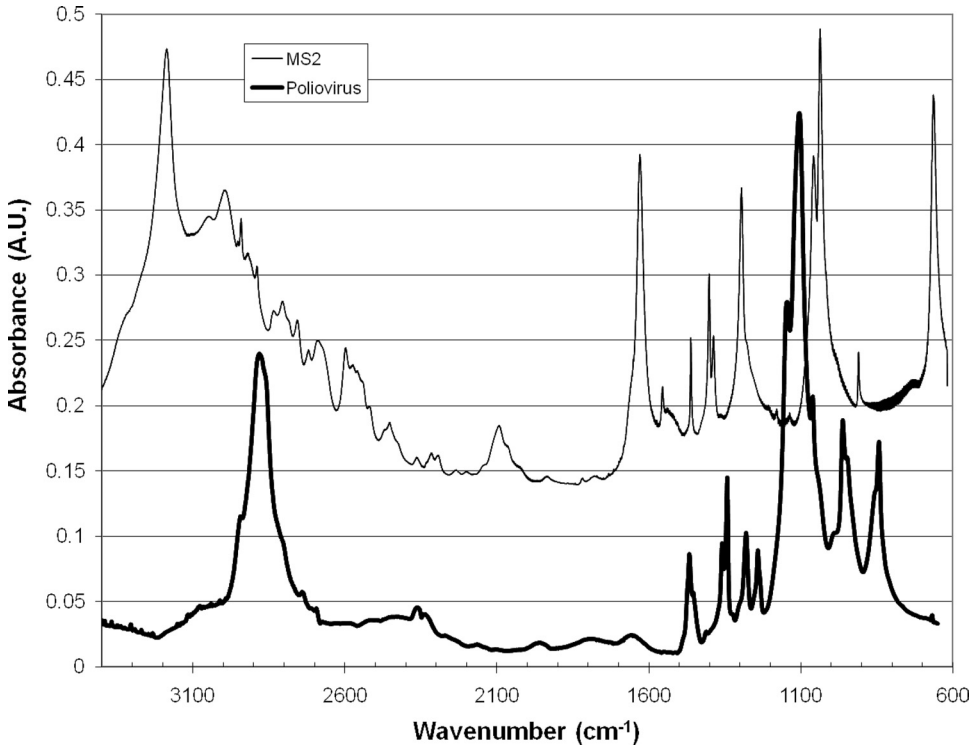

FIG. 3. Infrared spectra of dried MS2 and poliovirus collected as transmission measurements through Ge chips. Spectrum of MS2 has been baseline shifted for ease of interpretation by adding 0.14 to all points in the MS2 spectrum.

utilizing either protein-based feature. These provide the working range for protein measurements using transmission measurements for protein deposited on Ge chips.

Measurements of the poliovirus pipetted onto Ge chips (Fig. 5) showed a strong correlation between viral number and absorbance at 1,108 cm^{-1} (sugar) and 1,018 cm^{-1} (C—O acetate). Correlation coefficients were above 0.97 for each. These features correspond to virus-specific components and include

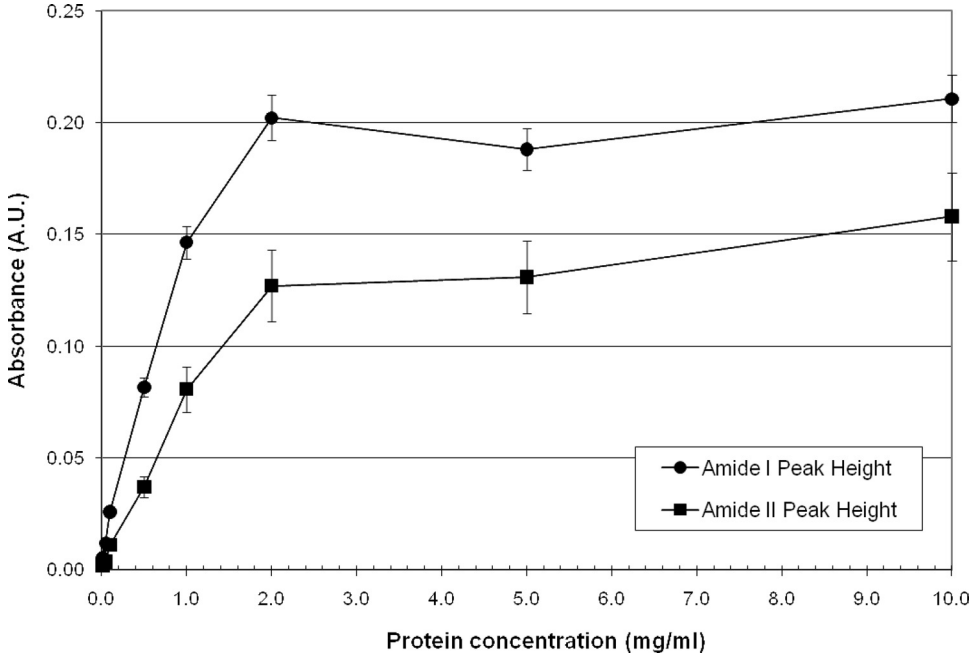

FIG. 4. Height of the amide I and amide II absorbance features for various concentrations of BSA deposited onto Ge chips. Protein is detectable with concentrations as little as 0.1 mg/ml.

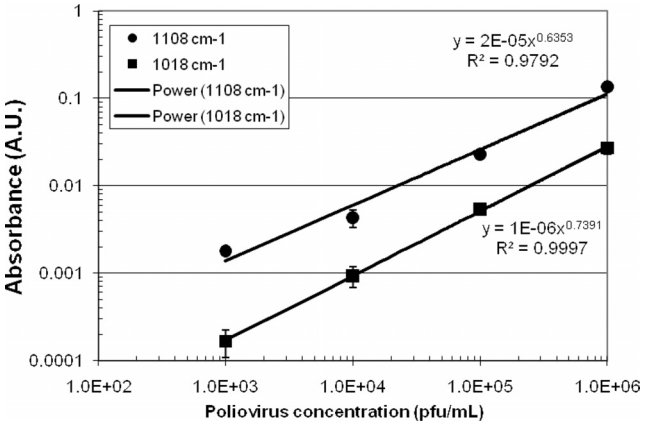

FIG. 5. Height of the sugar (1,108 cm^{-1}) and C—O acetate (1,018 cm^{-1}) absorbance features for various concentrations of poliovirus deposited onto Ge chips. Lines represent power law best fits to the data.

both infectious and noninfectious polioviruses. Under low-stress laboratory growth conditions, however, the poliovirus strain was found to have a relatively low particle:PFU ratio, approximately 10:1.

Figure 6a (BSA) and b (casein and lysozyme) provide a summary of amide I peak heights for electrodeposition of protein on the Ge chips over time and with various separation distances of 1 to 5 cm. Electrodeposition occurred predominantly within the first 10 min when the separation distance was less than 5 cm but required approximately 30 min when the separation distance was 5 cm. The cumulative amount of deposited protein depends on the protein type, its pI, and the separation distance. Larger amounts of protein are deposited with shorter separation distances. For the sake of clarity, only the 5-cm measurements are presented for casein and lysozyme; shorter separation distances generated very similar results with no substantial effect of separation distance.

Figure 6c shows the peak heights of amide I and amide II features of BSA deposited with a separation distance of 2 cm with various voltages from 0.5 to 5 V, with analysis performed at 30 min. Increasing the voltage appeared to decrease the peak intensity; however, differences were not statistically significant. The method utilizing Ge chips has inherently high variability, since each data point represents a separate experiment, each with its own protein solution. As before, the amide I feature was stronger than the amide II feature by approximately 50%; however, good correlation was apparent between these two features for any one experiment ($r^2 = 0.765$). A driving voltage of approximately 1 V was used in all subsequent experiments.

Figure 7 analyzes MS2 electrodeposited on Ge chips, assessed over 30 min using a 2-cm separation distance. Shown here is a summary of the peak absorbance heights for a number of virus-specific features (baseline corrected). MS2 deposition occurred quickly, with substantial deposition obtained within 5 min. Some features do show variability over time (1,542 and 1,656 cm^{-1}), with small decreases in peak height at intermediate times. The origin of this variability is not clear, but it is likely not due to release of MS2 into the solution, since not all features display this variability. Additionally, there were no

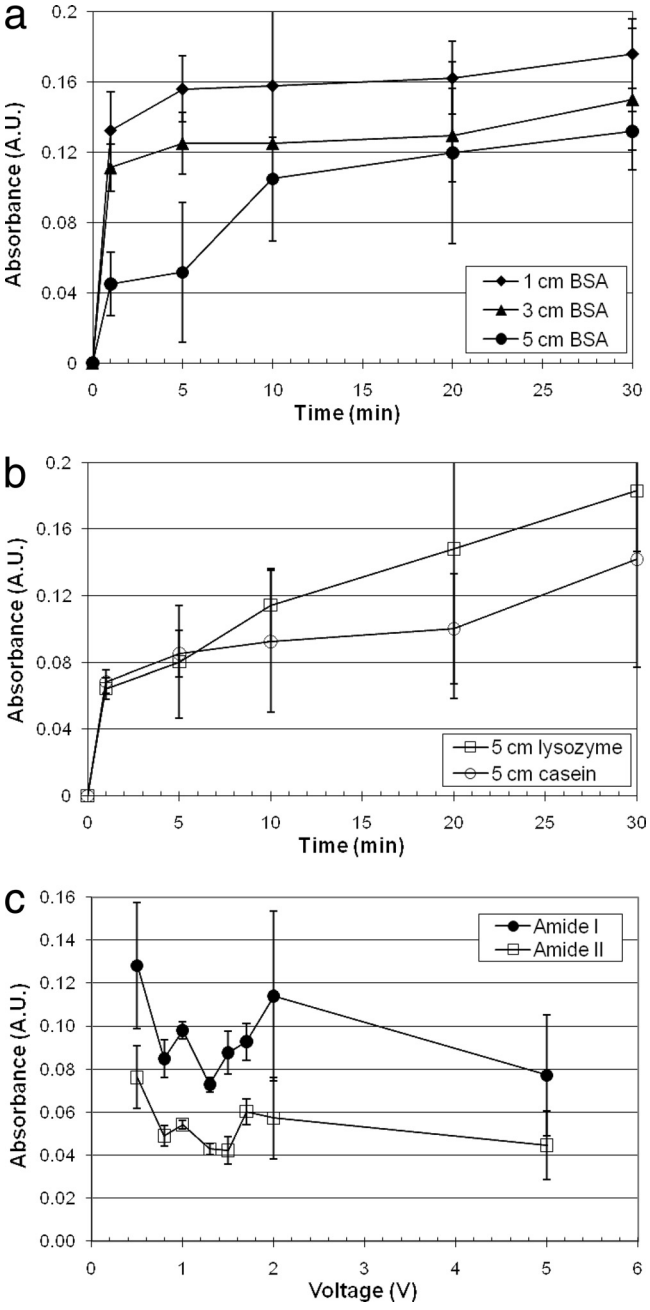

FIG. 6. (a) Protein-specific absorbance (amide I) after electrodeposition of BSA protein on Ge chips using 1.5 V and various times and separation distances. Error bars represent one standard deviation. (b) Protein-specific absorbance (amide I) after electrodeposition of protein (lysozyme or casein) on Ge chips using 1.5 V and various times and separation distances. Error bars represent one standard deviation. (c) Electrodeposition of BSA on Ge chips with a separation of 2 cm, voltage varied; analysis performed after 30 min.

apparent substantial alterations in virus chemistry, since spectra of electrodeposited virus closely matched that of pipetted virus. The sugar (1,038 cm^{-1}) and amide I protein (1,632 cm^{-1}) features appear to be the strongest indicators of virus capture and are features specific for MS2.

The electrodeposition of MS2 was also monitored in situ

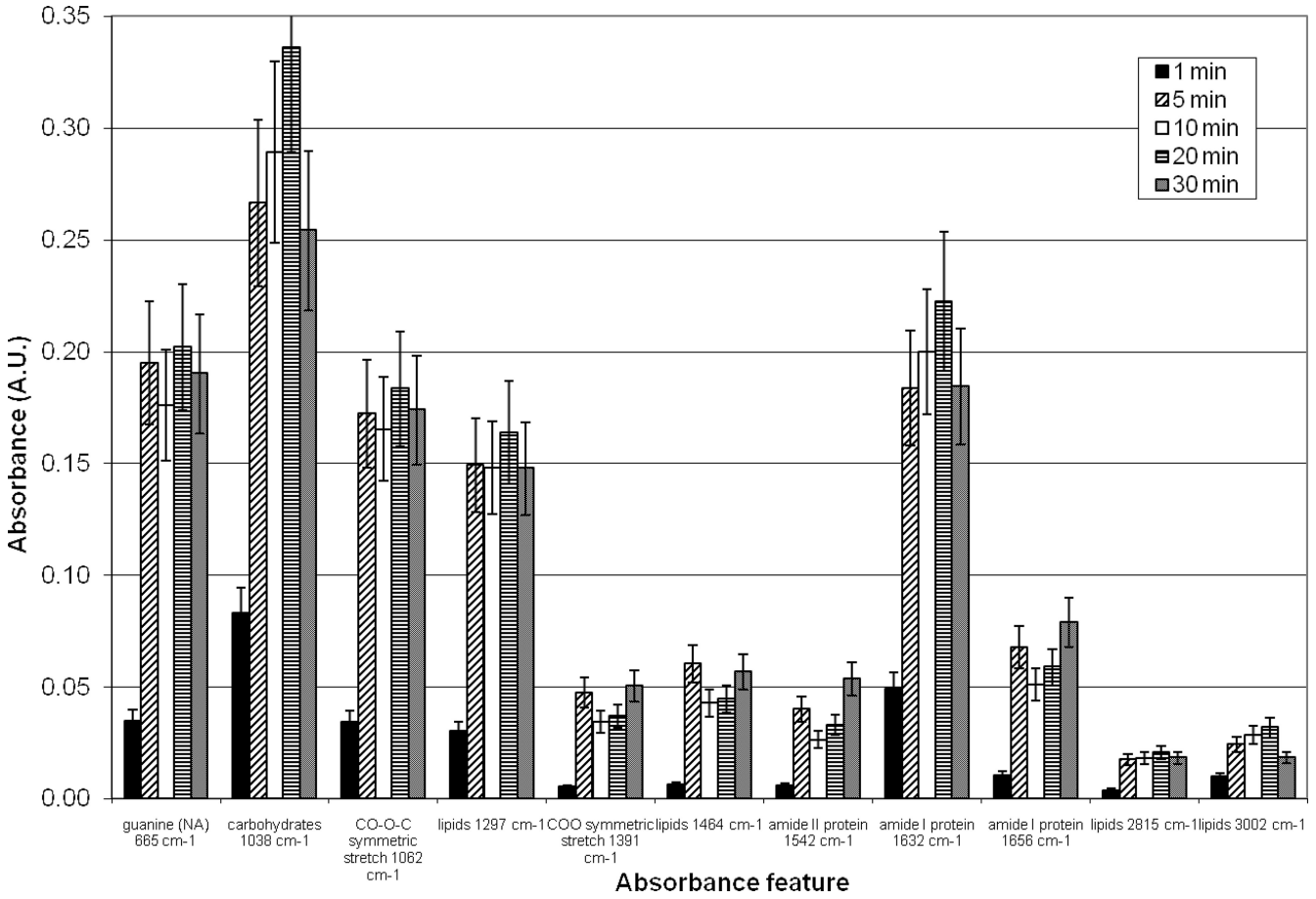

FIG. 7. Summary of MS2 absorbance features after electrodeposition on Ge chips for up to 30 min. Error bars represent the standard error of measurement with three replicates. The concentration of MS2 applied was 10^7 PFU/ml.

using an ATR crystal and a high-concentration bacteriophage solution made using tap water. Deposition of MS2 over time is shown in Fig. 8; four peaks show significant and consistent increases with time. The protein (amide I and amide II) features increased substantially over 50 min of deposition. Sugar and phosphate features showed a slower and more consistent rise over time. The protein absorbance features decreased significantly after 100 min of deposition.

Figure 9 shows a summary of peak heights for the electrodeposition of poliovirus onto an ATR crystal. Three spectral features were prominent for lipids (1,134 cm^{-1}), sugar (1,108 cm^{-1}), and nucleic acids/phospholipids (964 cm^{-1}). These each increased for at least the first 25 min of deposition. The nucleic acid features (964 cm^{-1}) increased slowly compared with the rise of the sugar (1,109 cm^{-1}) and lipid (1,134 cm^{-1}) features.

A question can be raised about the specificity of the species discrimination from the spectral features shown here after electrodeposition. Spectra collected using the ATR method do not perfectly match those from transmission measurements of fully dried biomass (which conventionally provide more distinct features). Figure 10 shows a comparison of electrodeposited poliovirus using ATR along with a transmission spectrum of dried poliovirus. The most distinct features were the broad band between 1,000 and 1,200 cm^{-1} and between 900 and 1,000 cm^{-1}. ATR spectral shapes (especially with fully hydrated samples) are commonly much broader than dried transmission spectra. The aforementioned features were the primary components that changed upon application of the voltage differential. Also shown in Fig. 10 is a spectrum of BGMK (buffalo green monkey kidney) cells taken in hydrated transmission. The BGMK cells represent the background found for susceptible cells used to grow these laboratory poliovirus stocks. Clearly the BGMK cells showed strong protein features that are not apparent in any of the poliovirus spectra. The poliovirus stocks were purified prior to use; these spectral differences provide evidence that little mammalian cell debris is depositing on the ATR surface during electrodeposition. Fully performing species analysis will require development of an extensive spectral database.

DISCUSSION

Presented here is a new approach for detection of viruses in drinking water. A voltage applied across an electrically conducting optical element is used to deposit charged materials with at least partial reversibility. An infrared spectroscopic measurement provides detection and discrimination of the

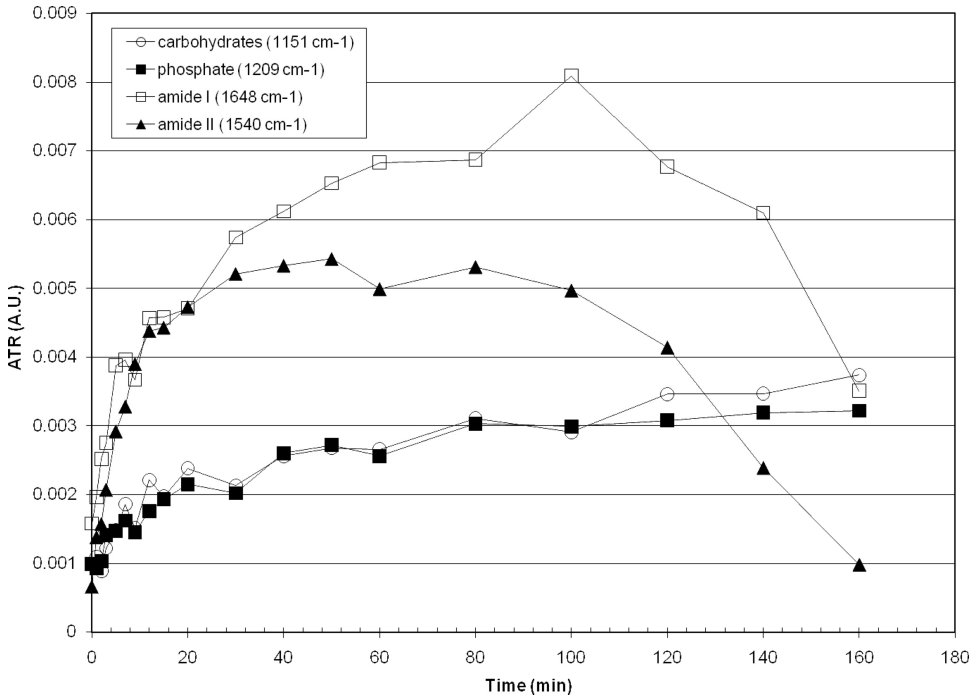

FIG. 8. Summary of four spectral features of MS2 electrodeposition on an ATR crystal.

types of materials that have been collected. Substantial differences are apparent in the infrared spectral features of three proteins and two viruses. These differences are sufficient to be used as the input for more sophisticated data analysis routines, such as principal component regression, principal component analysis, and partial least-squares regression, to be able to quantify individual components from within a complex of material deposited on the optical elements (27, 28, 32). Discussion

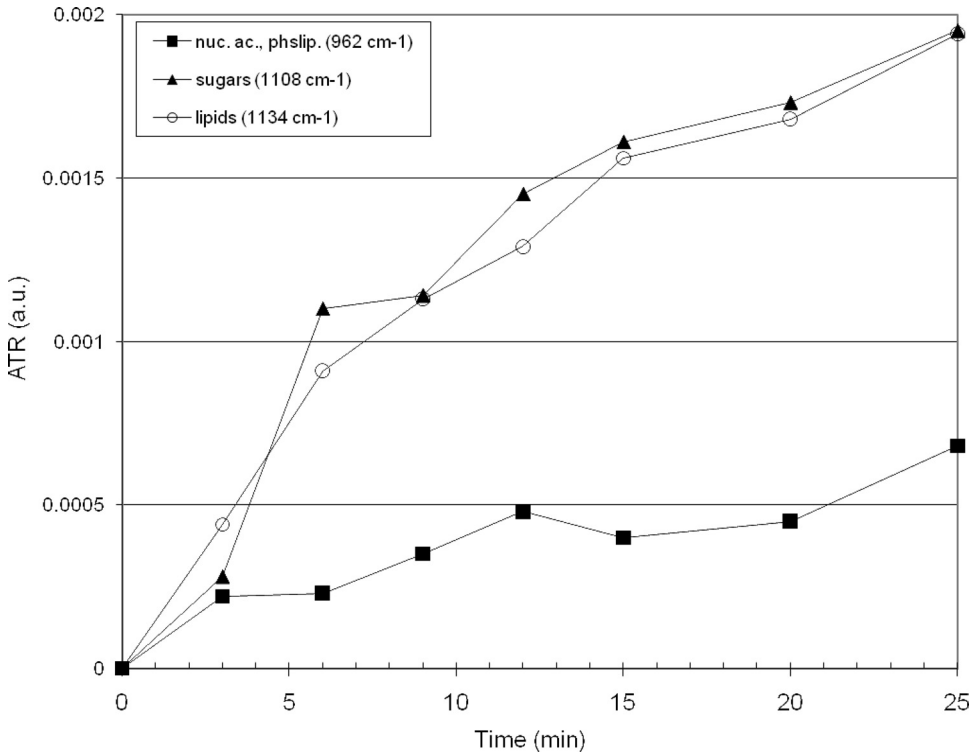

FIG. 9. Summary of poliovirus electrodeposition on ATR, showing three relevant spectral features. nuc. ac., nucleic acids; phslip., phospholipids.

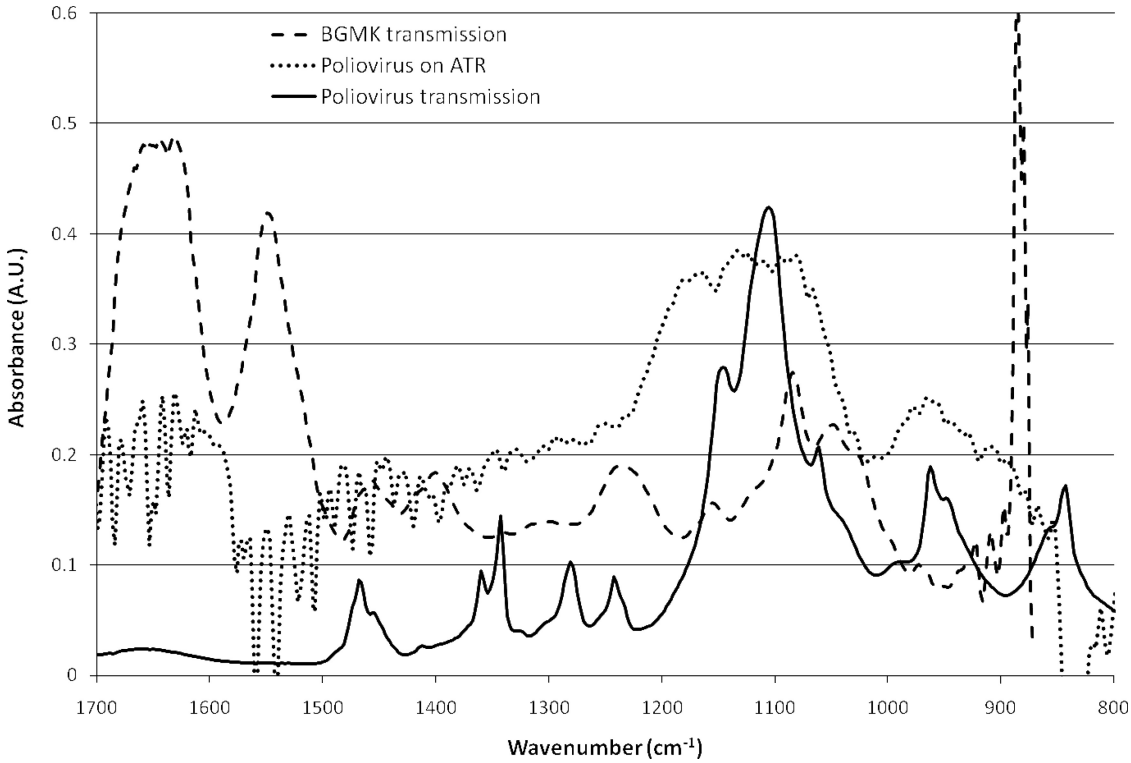

FIG. 10. Spectra of poliovirus deposited on the ATR crystal and through transmission measurements. Also shown is a transmission spectrum of BMGK cells, representing a typical background of cell debris that might be present in poliovirus stocks. Note that poliovirus stocks here were purified before use.

of these methods is beyond the scope of this article; however, reviews of the methods and demonstrations may be found in the references above.

All measurements here were made using tap water with added salts and pH adjustment but with no purification. This is a critical point for assessing the presented method, since any additional charged components present in the drinking water would similarly deposit on the ATR crystal. Even with variable water composition from day-to-day preparation, substantial spectral information was available to discriminate between three proteins and between two types of viruses. The drinking water in Tucson, AZ, for example, has high dissolved solids for a municipal supply and so presents a greater challenge for this measurement scheme than would likely be encountered in most municipal drinking water systems in urban areas.

Poliovirus and MS2 do not contain lipids. We have used the designation of a "lipid feature" since this is the typical designation for these molecular vibrations in the infrared. The signal derives from vibrations of CH_2 and CH_3 bonds which typically are found in lipids; however, their origin may reside in other biomolecules containing these common molecular structures. In order to be consistent with the infrared spectroscopy literature, we continue to use this "lipid feature" designation rather than attempting to develop a new identification for these molecular vibrations in poliovirus and MS2. The spectra in Fig. 10 display the spectral features that are distinct between poliovirus and a mammalian cell line and indicate that mammalian cell debris, with its high protein content, is not responsible for the signal increase with time of electrodeposition.

An advantage of this approach compared with molecular recognition techniques is that a wide variety of materials can be captured, delivered to the crystal surface, and assessed for spectral absorbance. Significant information is present within these spectra (20) to be able to perform discrimination between even closely related bacterial species (4, 8, 17). ATR works well for water-based measurements since the evanescent wave emanating from the crystal surface penetrates only approximate 1 μm into water (29). In this way, spectra are collected only from material that is in close contact with the crystal and is not interfered with by other materials suspended in solution. It is feasible to reverse the polarity of the driving voltage and so remove deposited compounds from the crystal surface (36). This provides a means to regenerate the crystal surface and continue measurements.

Figure 8 shows the increase in four spectral features for carbohydrates, phosphates, and protein (amide I and amide II) for MS2 electrodeposition on an ATR crystal. All four features displayed linear increases for the first 20 min, followed by a declining rate of deposition until approximately 80 min. At that time, these features no longer increase, and those for the protein decline from 100 min onward. This decrease in amide I and II features is likely due to unfolding of proteins within the viral capsid (34). Such unfolding is supported by a substantial degradation of components of the amide I and II features, indicative of a loss of protein secondary structure (α-helices, β-sheets, etc.), not shown. The sugar and phosphate features do not show such a decline and remain robust, thus suggesting

only a partial degradation in bacteriophage structure which does not release interior components.

Certainly the deposition process should be run for less than 60 min, since not only did the viral signal reach a plateau but no significant alteration in spectral features could be discerned between short-time (<60 min) electrodeposition and pipetted virus. Shorter time measurements are also necessary for practical aspects of measurements with a flowing water stream or perhaps to detect intentional additions of microorganisms to water systems. Measurement could be performed in as little as 5 min; longer deposition times could be used to search for lower-concentration contaminants.

Conclusions. The unique properties of the materials utilized here provide the capability to perform a simultaneous infrared spectroscopic measurement along with electrodeposition. The detection capability demonstrated here shows good sensitivity to low concentrations of pathogens, an ability to discriminate between pathogen type, and the potential for automated use. Reversibility, at least in a limited manner, is feasible but needs to be accomplished with greater removal of deposited materials. The device presented here is not suitable for online, continuous measurements but with small adjustments could be made to operate in the continual measurement scheme needed to ensure safety of drinking water.

Based on our results, significant deposition of two viruses (MS2 and poliovirus) can be observed after 5 min of operating time. While seemingly a long time for measurement in a flowing-water system, this is the same amount of time required for a number of commercial water monitoring systems in use in many municipalities already. Shorter times may be feasible with further development; however, the 5-min operation time would certainly be appropriate. The sensitivity obtained here is for a laboratory system designed to assess performance capabilities in a broad sense. Further development will likely decrease the detection limit. A comparison to laboratory-based methods (reverse transcription-PCR, etc.) is not appropriate since they are not automated for continual measurements and are not likely to be utilized for continuous 24/7 operation as is our method. The next steps in this work are to construct a sizeable spectral library of waterborne pathogens, to apply an online and continual measurement format, and to determine the limit of detection for such continual measurements.

ACKNOWLEDGMENTS

This work was supported by the University of Arizona BIO5 Institute and by the NIEHS-sponsored Southwest Environmental Health Sciences Center, grant no. P30 ES06694.

We gratefully acknowledge the assistance of Charles DeFer and the Agricultural and Biosystems Engineering Machine Shop.

REFERENCES

1. **Blackmer, F., K. A. Reynolds, C. P. Gerba, and I. L. Pepper.** 2000. Use of integrated cell culture-PCR to evaluate the effectiveness of poliovirus inactivation by chlorine. Appl. Environ. Microbiol. **66:**2267–2268.
2. **Bouzid, M., D. Steverding, and K. M. Tyler.** 2008. Detection and surveillance of waterborne protozoan parasites. Curr. Opin. Biotechnol. **19:**302–306.
3. **Davila, A. P., J. Jang, A. K. Gupta, T. Walter, A. Aronson, and R. Bashir.** 2007. Microresonator mass sensors for detection of *Bacillus anthracis* Sterne spores in air and water. Biosens. Bioelectron. **22:**3028–3035.
4. **Diem, M., M. Romeo, S. Boydston-White, M. Miljkovic, and C. Matthaus.** 2004. A decade of vibrational micro-spectroscopy of human cells and tissue (1994–2004). Analyst **129:**880–885.
5. **Garcia, A. A., M. R. Bonen, J. Ramirez-Vick, M. Sadaka, and A. Vuppu.** 1999. Bioseparation process science. Blackwell Science, Inc., Malden, MA.
6. **Gerba, C. P.** 1984. Applied and theoretical aspects of virus adsorption to surfaces. Adv. Appl. Microbiol. **30:**133–168.
7. **Goeller, L. J., and M. R. Riley.** 2007. Discrimination of bacteria and bacteriophages by Raman spectroscopy and surface enhanced Raman spectroscopy. Appl. Spectrosc. **6:**1–7.
8. **Helm, D., and D. Naumann.** 1995. Identification of some bacterial cell components by FT-IR spectroscopy. FEMS Microbiol. Lett. **126:**75–80.
9. **Leonard, P., S. Hearty, J. Brennan, L. Dunne, J. Quinn, T. Chakraborty, and R. O'Kennedy.** 2003. Advances in biosensors for detection of pathogens in food and water. Enzyme Microb. Technol. **32:**3–13.
10. **Lucas, P., M. A. Solis, D. Le Coq, C. Juncker, M. R. Riley, J. Collier, D. E. Boesewetter, C. Boussard-Plédel, and B. Bureau.** 2005. Infrared biosensors using hydrophobic chalcogenide fibers sensitized with live cells. Sens. Actuators B **119:**355–362.
11. **Lucas, P., M. R. Riley, M. A. Solis, C. Juncker, J. Collier, and D. E. Boesewetter.** 2005. Hydrophobic chalcogenide fibers for cell-based bio-optical sensors. *In* I. Gannot (ed.), Optical fibers and sensors for medical applications. Proc. SPIE, vol. 5691, p. 104–114.
12. **Lucas, P., D. Le Coq, J. M. Collier, D. E. Boesewetter, C. Boussard-Pledel, B. Bureau, and M. R. Riley.** 2005. Evaluation of toxic agent effects on lung cells by fiber evanescent wave spectroscopy (FEWS). Appl. Spectrosc. **59:**1–9.
13. **Lucas, P., M. R. Riley, C. Boussard-Plédel, and B. Bureau.** 2006. Advances in chalcogenide fibers evanescent-wave biochemical sensing. Anal. Biochem. **351:**1–10.
14. **Lucas, P., M. A. Solis, D. Le Coq, C. Juncker, M. R. Riley, J. Collier, D. E. Boesewetter, C. Boussard-Plédel, and B. Bureau.** 2006. Spectroscopic properties of chalcogenide fibers for bio-sensor applications. Phys. Chem. Glasses **47:**88–91.
15. **Lucas, P., A. A. Wilhelm, M. Videa, C. Boussard-Plédel, and B. Bureau.** 2008. Chemical stability of chalcogenide infrared glass fibers. Corros. Sci. **50:**2047–2052.
16. **Lukasik, J., T. M. Scott, D. Andryshak, and S. R. Farrah.** 2000. Influence of salts on virus adsorption to microporous filters. Appl. Environ. Microbiol. **66:**2914–2920.
17. **Naumann, D.** 2000. Infrared spectroscopy in microbiology, p. 102–131. *In* R. A. Meyers (ed.), Encyclopedia of analytical chemistry. John Wiley & Sons Ltd., Chichester, United Kingdom.
18. **Ngo-Thi, N. A., C. Kirschner, and D. Naumann.** 2003. Characterization and identification of microorganisms by FT-IR microspectrometry. J. Mol. Struct. **661–662:**371–380.
19. **Penrod, S. L., T. M. Olson, and S. B. Grant.** 1995. Whole particle microelectrophoresis for small viruses. J. Colloid Interface Soc. **173:**521–523.
20. **Petibois, C., K. Gionnet, M. Goncalves, A. Perromat, M. Moenner, and G. Deleris.** 2006. Analytical performances of FT-IR spectrometry and imaging for concentration measurements within biological fluids, cells, and tissues. Analyst **131:**640–647.
21. **Redman, J. A., S. B. Grant, T. M. Olson, and M. K. Estes.** 2001. Pathogen filtration, heterogeneity, and the potable reuse of wastewater. Environ. Sci. Technol. **35:**1798–1805.
22. **Reynolds, K. A., C. P. Gerba, and I. L. Pepper.** 1996. Detection of infectious enteroviruses using an integrated cell culture/PCR procedure. Appl. Environ. Microbiol. **62:**1424–1427.
23. **Reynolds, K. A., K. Roll, R. S. Fujioka, C. P. Gerba, and I. L. Pepper.** 1998. Incidence of enteroviruses in Mamala Bay, Hawaii using cell culture and direct polymerase chain reaction methodologies. Can. J. Microbiol. **44:**598–604.
24. **Reynolds, K. A., C. P. Gerba, M. Abbaszadegan, and I. L. Pepper.** 2001. ICC/PCR detection of enteroviruses and hepatitis A virus in environmental samples. Can. J. Microbiol. **47:**153–157.
25. **Rigas, B., S. Morgello, I. S. Goldman, and P. T. T. Wong.** 1990. Human colorectal cancers display abnormal Fourier-transform infrared spectra. Proc. Natl. Acad. Sci. USA **87:**8140–8144.
26. **Riley, M. R., C. D. Okeson, and B. L. Frazier.** 1999. Rapid calibration development for near infrared spectroscopic monitoring of mammalian cell cultivations. Biotechnol. Prog. **15:**1133–1141.
27. **Riley, M. R., and H. M. Crider.** 2000. The effect of analyte concentration range on measurement errors obtained by NIR spectroscopy. Talanta **52:**473–484.
28. **Riley, M. R., H. M. Crider, M. E. Nite, R. A. Garcia, J. Woo, and R. M. Wegge.** 2001. Simultaneous measurement of 19 components in animal cell culture media by near infrared spectroscopy. Biotechnol. Progr. **17:**376–378.
29. **Riley, M. R., P. Lucas, D. Le Coq, J. M. Collier, D. E. Boesewetter, D. M. DeRosa, M. E. Katterman, C. Boussard-Plédel, and B. Bureau.** 2006. Lung cell fiber evanescent wave spectroscopic biosensing of inhalation health hazards. Biotechnol. Bioeng. **95:**599–612.
30. **Riley, M. R., D. L. DeRosa, J. Blaine, B. G. Potter, Jr., P. Lucas, D. Le Coq, C. Juncker, D. E. Boesewetter, J. M. Collier, C. Boussard-Plédel, and B. Bureau.** 2006. Biologically-inspired sensing: infrared spectroscopic analysis of cell responses to inhalation health hazards. Biotechnol. Progr. **22:**24–31.
31. **Ryan, J. N., R. W. Harvey, D. Metge, M. Elimelech, T. Navigato, and A. P. Pieper.** 2002. Field and laboratory investigations of inactivation of viruses

(PRD1 and MS2) attached to iron oxide-coated quartz sand. Environ. Sci. Technol. **36:**2403–2413.
32. **Sakudo, A., Y. Suganuma, T. Kobayashi, T. Onodera, and K. Ikuta.** 2006. Near-infrared spectroscopy: promising diagnostic tool for viral infections. Biochem. Biophys. Res. Commun. **341:**279–284.
33. **Schaldach, C. M., W. L. Bourcier, H. F. Shaw, B. E. Viani, and W. D. Wilson.** 2006. The influence of ionic strength on the interaction of viruses with charged surfaces under environmental conditions. J. Colloid Interface Sci. **294:**1–10.
34. **Wang, L.-X., F. Meersman, and Y. Wu.** 2008. A principal component analysis and two-dimensional correlation infrared spectroscopy study on the thermal unfolding of ribonuclease A under reducing conditions. J. Mol. Struct. **883–884:**79–84.
35. **Wilhelm A. A., P. Lucas, D. L. DeRosa, and M. R. Riley.** 2007. Biocompatibility of chalcogenide fibers for cell-based optical sensing. J. Mater. Res. **22:**1098–1104.
36. **Wilhelm, A. A., P. Lucas, K. Reynolds, and M. R. Riley.** 2008. Integrated capture and spectroscopic detection of viruses in an aqueous environment. *In* Optical fibers and sensors for medical diagnostics and treatment applications VIII. Proc. SPIE, vol. 6852, p. 1–8.
37. **Yoder, J., V. Roberts, G. F. Craun, V. Hill, L. Hicks, N. T. Alexander, V. Radke, R. L. Calderon, M. C. Hlavsa, M. J. Beach, and S. L. Roy.** 2008. Surveillance for waterborne disease and outbreaks associated with drinking water and water not intended for drinking—United States, 2005–2006. MMWR Morb. Mort. Wkly. Rep. **57:**39–62.